

VARIABLE EXPONENT, LINEAR GROWTH FUNCTIONALS IN
IMAGE RESTORATION*YUNMEI CHEN[†], STACEY LEVINE[‡], AND MURALI RAO[†]

Abstract. We study a functional with variable exponent, $1 \leq p(x) \leq 2$, which provides a model for image denoising, enhancement, and restoration. The diffusion resulting from the proposed model is a combination of total variation (TV)-based regularization and Gaussian smoothing. The existence, uniqueness, and long-time behavior of the proposed model are established. Experimental results illustrate the effectiveness of the model in image restoration.

Key words. image restoration, linear growth functionals, variable exponent, BV-space, Dirichlet boundary condition

AMS subject classifications. 49J40, 35K65

DOI. 10.1137/050624522

1. Introduction.

1.1. Background. In this paper we propose a new model for image restoration. In the version we address, an image, u , is recovered from an observed, noisy image, I , where the two are related by $I = u + noise$. The proposed model incorporates the strengths of the various types of diffusion arising from the minimization problem

$$(1.1) \quad \min \int_{\Omega} |Du|^p + \frac{\lambda}{2}(u - I)^2$$

for $1 \leq p \leq 2$ ($\lambda \geq 0$, and Ω is an open, bounded subset of \mathbb{R}^n with Lipschitz boundary). Specifically, we exploit the benefits of isotropic diffusion ($p = 2$), total variation (TV)-based diffusion ($p = 1$), and more general anisotropic diffusion ($1 < p < 2$).

TV minimization, $p = 1$. TV-based regularization, $p = 1$, as first proposed by Rudin, Osher, and Fatemi [31], does an excellent job of preserving edges while reconstructing images. Mathematically this is reasonable, since it is natural to study solutions of this problem in the space of functions of bounded variation, $BV(\Omega)$, allowing for discontinuities which are necessary for edge reconstruction. This phenomenon can also be explained physically, since the resulting diffusion is strictly orthogonal to the gradient of the image. The TV model has been studied extensively (see, e.g., [1, 15]) and has proved to be an invaluable tool for preserving sharp edges.

*Received by the editors February 15, 2005; accepted for publication (in revised form) December 12, 2005; published electronically May 3, 2006. The first and third authors were supported in part by NIH R01 NS42075. The second author was supported in part by NSF DMS 0505729.

[†]<http://www.siam.org/journals/siap/66-4/62452.html>

[‡]Department of Mathematics, P.O. Box 118505, University of Florida, Gainesville, FL 32611 (yun@math.ufl.edu, rao@math.ufl.edu).

[‡]Department of Mathematics and Computer Science, Duquesne University, Pittsburgh, PA 15282 (sel@mathcs.duq.edu).

Given the success of TV-based diffusion, various modifications have been introduced. For instance, Strong and Chan [32] proposed the adaptive total variation model

$$\min \int_{\Omega} \alpha(x) |\nabla u|$$

in which they introduce a control factor, $\alpha(x)$, which slows the diffusion at likely edges. This controls the *speed* of the diffusion and has demonstrated good results, as it aids in noise reduction. It is also good at reconstructing edges, since the *type* of diffusion (strictly orthogonal to the image gradient) is the same as that of the original TV model.

TV-based denoising favors solutions that are piecewise constant. This sometimes causes a *staircasing* effect in which noisy smooth regions are processed into piecewise constant regions (see Figure 5.1), a phenomenon long observed in the literature; see, e.g., [9, 15, 20, 28, 30, 34, 36]. Not only do “blocky” solutions fail to satisfy the ubiquitous “eyeball norm,” but they can also develop “false edges,” which can mislead a human or computer into identifying erroneous features not present in the true image.

Minimization problem (1.1) with $1 < p \leq 2$. On the other hand, one can explore different *types* of diffusion arising from (1.1). Choosing $p = 2$ results in isotropic diffusion, which solves the staircasing problem but alone is not good for image reconstruction since it has no mechanism for preserving edges. Different values of $1 < p < 2$ result in anisotropic diffusion, which is somewhere between TV-based and isotropic smoothing. This type of diffusion can be effective in reconstructing piecewise smooth regions. However, a fixed value of $1 < p < 2$ may not allow for discontinuities, thus obliterating edges. This was shown to be true in the discrete case [28].

Combination of TV-based and isotropic diffusion. Given the strengths of (1.1) for different values of p , it seems worthwhile to investigate a model which could self-adjust in order to reap the benefits of each type of diffusion. To this end, Chambolle and Lions [15] proposed minimizing the following energy functional, which combines isotropic and TV-based diffusion:

$$(1.2) \quad \min_{u \in BV(\Omega)} \frac{1}{2\beta} \int_{|\nabla u| \leq \beta} |\nabla u|^2 + \int_{|\nabla u| > \beta} |\nabla u| - \frac{\beta}{2}.$$

In this model, the diffusion is strictly perpendicular to the gradient, where $|\nabla u| > \beta$, that is, where edges are most likely present, and isotropic where $|\nabla u| \leq \beta$. This model is successful in restoring images in which homogeneous regions are separated by distinct edges; however, if the image intensities representing objects are nonuniform, or if an image is highly degraded, this model may become sensitive to the threshold, β (see Figures 5.2, 5.3, and 5.4). In this case, one might want more flexibility when choosing both the direction and speed of diffusion.

Blomgren et al. [9] proposed the minimization problem

$$\min \int_{\Omega} |\nabla u|^{p(|\nabla u|)} dx,$$

where $\lim_{s \rightarrow 0} p(s) = 2$, $\lim_{s \rightarrow \infty} p(s) = 1$, and p is monotonically decreasing. This model should reap the benefits of both isotropic and TV-based diffusion, as well as a combination of the two. However, it is difficult to study mathematically since the lower semicontinuity of the functional is not readily evident.

1.2. Functionals with variable exponent $1 \leq p(x) \leq 2$. The model proposed in this paper capitalizes on the strengths of (1.1) for the different values of $1 \leq p \leq 2$. It ensures TV-based diffusion ($p \equiv 1$) along edges and Gaussian smoothing ($p \equiv 2$) in homogeneous regions. Furthermore, it employs anisotropic diffusion ($1 < p < 2$) in regions which may be piecewise smooth or in which the difference between noise and edges is difficult to distinguish. We let $p = p(x)$ depend on the location, x , in the image. This way, the direction and speed of diffusion at each location depend on the local behavior. Moreover, our choice of exponent yields a model which we can show is theoretically sound.

To this end, the proposed model is as follows:

$$(1.3) \quad \min_{u \in BV \cap L^2(\Omega)} \int_{\Omega} \phi(x, Du) + \frac{\lambda}{2}(u - I)^2,$$

where

$$(1.4) \quad \phi(x, r) := \begin{cases} \frac{1}{q(x)} |r|^{q(x)}, & |r| \leq \beta, \\ |r| - \frac{\beta q(x) - \beta^{q(x)}}{q(x)}, & |r| > \beta, \end{cases}$$

where $\beta > 0$ is fixed and $1 < \alpha \leq q(x) \leq 2$. For instance, one can choose

$$(1.5) \quad q(x) = 1 + \frac{1}{1 + k|\nabla G_{\sigma} * I(x)|^2},$$

where $G_{\sigma}(x) = \frac{1}{\sigma} \exp(-|x|^2/4\sigma^2)$ is the Gaussian filter and $k > 0$ and $\sigma > 0$ are fixed parameters.

The main benefit of (1.3)–(1.4) is the manner in which it accommodates the local image information. Where the gradient is sufficiently large (i.e., at likely edges), only TV-based diffusion will be used. Where the gradient is close to zero (i.e., in homogeneous regions), the model is isotropic. At all other locations, the filtering is somewhere between Gaussian and TV-based diffusion. Specifically, the type of anisotropy at these ambiguous regions varies according to the strength of the gradient. This enables the model to have a much lower dependence on the threshold (see Figures 5.2, 5.3, 5.4, and 5.5).

For several reasons, we've chosen here to prove the well-posedness of the Dirichlet boundary value problem

$$(1.6) \quad \min_{u \in BV_g \cap L^2(\Omega)} \int_{\Omega} \phi(x, Du) + \frac{\lambda}{2}(u - I)^2,$$

where

$$(1.7) \quad BV_g(\Omega) := \{u \in BV(\Omega) | u = g \text{ on } \partial\Omega\},$$

and its associated flow

$$(1.8) \quad \dot{u} - \operatorname{div}(\phi_r(x, Du)) + \lambda(u - I) = 0 \quad \text{in } \Omega^T,$$

$$(1.9) \quad u(x, t) = g(x) \quad \text{on } \partial\Omega^T,$$

$$(1.10) \quad u(0) = I \quad \text{in } \Omega,$$

where

$$(1.11) \quad \Omega^T := \Omega \times [0, T] \quad \text{and} \quad \partial\Omega^T := \partial\Omega \times [0, T].$$

First, the theory is more interesting and challenging mathematically than (1.3). Second, all of the techniques used to study (1.6) also directly solve (1.3). Finally, the Dirichlet problem (1.6) also has direct application in image processing, as it can be used for image interpolation [13, 27], also referred to as noise-free image inpainting [8, 17, 18].

For a special case of (4), where $q(x) \equiv 2$, i.e., $\phi(r) := |r| - \frac{1}{2}$ when $|r| > 1$ and $\phi(r) := \frac{1}{2}|r|^2$ when $|r| \leq 1$, the existence, uniqueness, and long-time behavior of solutions of (1.6) and its related flow were studied by Zhou [37]. Later, these results were extended to general convex linear-growth functionals, $\phi = \phi(Du)$, by Hardt and Zhou [23]. In this paper we study the more general case, where the functional has a variable exponent and where $\phi = \phi(x, Du)$. We use a different approximate functional than [37], so different estimates are required. Our analysis is also based on techniques introduced in [19]; however, our energy functional requires alternate techniques to establish lower semicontinuity and to pass to the limit from the approximate solution. More related work on linear-growth functionals and their flows can be found in [2, 3, 4, 5, 6, 7, 12, 14, 33]. We also refer the reader to the work in [15, 16, 26, 35] for an alternate variational approach for reducing staircasing by minimizing second order functionals.

The paper is organized as follows. In section 2 we establish some important properties of $\phi(x, Du)$. In section 3 we prove the existence and uniqueness of the solution of minimization problem (1.6). In section 4 we study the associated evolution problem (1.8)–(1.10). Specifically, we define the notion of a weak solution of (1.8)–(1.10), derive estimates for the solution of an approximating problem, prove existence and uniqueness of the solution of (1.8)–(1.10), and discuss the behavior of the solution as $t \rightarrow \infty$. In section 5 we provide our numerical algorithm and experimental results to illustrate the effectiveness of our model in image restoration.

2. Properties of ϕ . Recall that for $u \in BV(\Omega)$,

$$Du = \nabla u \cdot \mathcal{L}^n + D^s u$$

is a Radon measure, where ∇u is the density of the absolutely continuous part of Du with respect to the n -dimensional Lebesgue measure, \mathcal{L}^n , and $D^s u$ is the singular part (see [21]).

DEFINITION 2.1. For $v \in BV(\Omega)$, define

$$\int_{\Omega} \phi(x, Dv) := \int_{\Omega} \phi(x, \nabla v) dx + \int_{\Omega} |D^s v|,$$

where ϕ is defined as in (1.4). Furthermore, denote

$$(2.1) \quad \Phi_{\lambda}(v) := \int_{\Omega} \phi(x, Dv) + \frac{\lambda}{2} \int_{\Omega} |v - I|^2 dx,$$

$$(2.2) \quad \Phi_g(v) := \int_{\Omega} \phi(x, Dv) + \int_{\partial\Omega} |v - g| d\mathcal{H}^{n-1},$$

and

$$(2.3) \quad \Phi_{\lambda,g}(v) := \int_{\Omega} \phi(x, Dv) + \frac{\lambda}{2} \int_{\Omega} |v - I|^2 dx + \int_{\partial\Omega} |v - g| d\mathcal{H}^{n-1}.$$

Remark 2.2. For simplicity, we assume that the threshold $\beta = 1$ in (1.4) for all of our theoretical results.

Similarly to the idea of [10, 11], we can establish lower semicontinuity of the functional Φ_g . For the convenience of the reader, we include the proof below.

LEMMA 2.3. *Using the notation in Definition 2.1,*

$$(2.4) \quad \Phi_g(u) = \tilde{\Phi}_g(u)$$

for all $u \in BV(\Omega)$, where

$$\tilde{\Phi}_g(u) := \sup_{\substack{\psi \in C^1(\bar{\Omega}, \mathbb{R}^n) \\ |\psi| \leq 1}} \int_{\Omega} -u \operatorname{div} \psi - \frac{q(x)-1}{q(x)} |\psi|^{\frac{q(x)}{q(x)-1}} dx + \int_{\partial\Omega} \psi \cdot n g d\mathcal{H}^{n-1}.$$

Furthermore, $\Phi_g(u)$ is lower semicontinuous on $L^1(\Omega)$; that is, if $u_j, u \in BV(\Omega)$ satisfy $u_j \rightarrow u$ in $L^1(\Omega)$ as $j \rightarrow \infty$, then $\Phi_g(u) \leq \liminf_{j \rightarrow \infty} \Phi_g(u_j)$.

Proof. For each $\psi \in C^1(\bar{\Omega}, \mathbb{R}^n)$, the map $u \rightarrow \int_{\Omega} -u \operatorname{div} \psi - \frac{q(x)-1}{q(x)} |\psi|^{\frac{q(x)}{q(x)-1}} dx + \int_{\partial\Omega} \psi \cdot n g d\mathcal{H}^{n-1}$ is continuous and affine on $L^1(\Omega)$. Therefore, $\tilde{\Phi}_g(u)$ is convex and lower semicontinuous on $L^1(\Omega)$ and the domain of $\tilde{\Phi}_g(u)$, $\{u \mid \tilde{\Phi}_g(u) < \infty\}$, is precisely $BV(\Omega)$.

We now show that $\Phi_g(u) = \tilde{\Phi}_g(u)$. For $u \in BV(\Omega)$, we have that for each $\psi \in C^1(\bar{\Omega}, \mathbb{R}^n)$,

$$-\int_{\Omega} u \operatorname{div} \psi dx = \int_{\Omega} \nabla u \cdot \psi dx + \int_{\Omega} D^s u \cdot \psi - \int_{\partial\Omega} u \psi \cdot n d\mathcal{H}^{n-1}.$$

Therefore, since the measures dx , $D^s u$, and $d\mathcal{H}^{n-1}$ are mutually singular, standard arguments show that

$$\tilde{\Phi}_g(u) = \sup_{\substack{\psi \in C^1(\bar{\Omega}, \mathbb{R}^n) \\ |\psi| \leq 1}} \int_{\Omega} \nabla u \cdot \psi - \frac{q(x)-1}{q(x)} |\psi|^{\frac{q(x)}{q(x)-1}} dx + \int_{\Omega} |D^s u| + \int_{\partial\Omega} |u - g| d\mathcal{H}^{n-1}.$$

The proof is then complete once we establish that

$$(2.5) \quad \int \phi(x, \nabla u) dx = \sup_{\substack{\psi \in C^1(\bar{\Omega}, \mathbb{R}^n) \\ |\psi| \leq 1}} \int \nabla u \cdot \psi - \frac{q(x)-1}{q(x)} |\psi|^{\frac{q(x)}{q(x)-1}} dx.$$

Since any $\rho \in L^\infty(\Omega, \mathbb{R}^n)$ can be approximated in measure by $\psi \in C^1(\bar{\Omega}, \mathbb{R}^n)$, we have that

$$(2.6) \quad \sup_{\substack{\psi \in C^1(\bar{\Omega}, \mathbb{R}^n) \\ |\psi| \leq 1}} \int_{\Omega} \nabla u \cdot \psi - \frac{q(x)-1}{q(x)} |\psi|^{\frac{q(x)}{q(x)-1}} dx = \sup_{\substack{\rho \in L^\infty(\Omega, \mathbb{R}^n) \\ |\rho| \leq 1}} \int_{\Omega} \nabla u \cdot \rho - \frac{q(x)-1}{q(x)} |\rho|^{\frac{q(x)}{q(x)-1}} dx.$$

Choosing $\rho(x) = 1_{\{|\nabla u| \leq 1\}} |\nabla u|^{q(x)-1} \frac{\nabla u}{|\nabla u|} + 1_{\{|\nabla u| > 1\}} \frac{\nabla u}{|\nabla u|}$, where 1_E is the indicator function on E , we see that the right-hand side of (2.6) is

$$(2.7) \quad \geq \int_{\Omega} \frac{1}{q(x)} |\nabla u|^{q(x)} 1_{\{|\nabla u| \leq 1\}} + \left[|\nabla u| - \frac{q(x)-1}{q(x)} \right] 1_{\{|\nabla u| > 1\}} dx = \int_{\Omega} \phi(x, \nabla u) dx.$$

To show equality in (2.5), we proceed as follows. For any $\rho \in L^\infty(\Omega, \mathbb{R}^n)$, since $q(x) > 1$ we have that for almost all x , $\nabla u(x) \cdot \rho(x) \leq \frac{1}{q(x)} |\nabla u|^{q(x)} + \frac{q(x)-1}{q(x)} |\rho(x)|^{\frac{q(x)}{q(x)-1}}$. In particular, if $|\nabla u| \leq 1$,

$$(2.8) \quad \nabla u(x) \cdot \rho(x) - \frac{q(x)-1}{q(x)} |\rho(x)|^{\frac{q(x)}{q(x)-1}} \leq \frac{1}{q(x)} |\nabla u|^{q(x)}.$$

On the other hand, if $|\nabla u| > 1$ and $|\rho| \leq 1$, then since $q(x) > 1$ for almost all x , we have that $\nabla u \cdot \rho = |\nabla u| \frac{\nabla u}{|\nabla u|} \cdot \rho \leq |\nabla u| \left[\frac{1}{q(x)} + \frac{q(x)-1}{q(x)} |\rho|^{\frac{q(x)}{q(x)-1}} \right]$, and thus

$$(2.9) \quad \begin{aligned} \nabla u \cdot \rho - \frac{q(x)-1}{q(x)} |\rho|^{\frac{q(x)}{q(x)-1}} &\leq \frac{1}{q(x)} |\nabla u| + (|\nabla u| - 1) \frac{q(x)-1}{q(x)} |\rho|^{\frac{q(x)}{q(x)-1}} \\ &\leq |\nabla u| - \frac{q(x)-1}{q(x)}. \end{aligned}$$

Combining (2.6), (2.7), (2.8), and (2.9), we have that

$$\sup_{\substack{\psi \in C^1(\overline{\Omega}, \mathbb{R}^n) \\ |\psi| \leq 1}} \int_{\Omega} \nabla u \cdot \psi - \frac{q(x)-1}{q(x)} |\psi|^{\frac{q(x)}{q(x)-1}} dx = \int_{\Omega} \phi(x, \nabla u) dx,$$

and thus for all $u \in BV(\Omega)$, $\tilde{\Phi}_g(u) = \Phi_g(u)$, where Φ_g is defined as in (2.2). \square

LEMMA 2.4. *Suppose $\Omega \subset \mathbb{R}^n$ is open, bounded, and has Lipschitz boundary, and let $w \in BV \cap L^2(\Omega)$. Then for each $\delta > 0$, there exists $\tilde{w}_\delta \in C^\infty \cap H^1(\Omega)$ such that*

$$(2.10) \quad \|\tilde{w}_\delta - w\|_{L^2(\Omega)} \leq \delta$$

and

$$(2.11) \quad \Phi_{\lambda,g}(\tilde{w}_\delta) \leq \Phi_{\lambda,g}(w) + \delta.$$

Furthermore, if we also assume that $Trw = TrG$ on $\partial\Omega$ for some $G \in H^1(\Omega)$, then for each $\delta > 0$, there exists $w_\delta \in H^1(\Omega)$ satisfying

$$(2.12) \quad Trw_\delta = Trw \quad \text{on } \partial\Omega,$$

$$(2.13) \quad w_\delta \rightarrow w \quad \text{strongly in } L^2(\Omega) \quad \text{as } \delta \rightarrow 0,$$

and

$$(2.14) \quad \Phi_{\lambda,g}(w_\delta) \leq \Phi_{\lambda,g}(w) + \delta,$$

where TrG is the trace of G on $\partial\Omega$.

Proof. Fix $w \in BV \cap L^2(\Omega)$. Using Lemma 2.3 and a slight modification of the proof of Theorem 1.17 and Remark 1.18 in [22], there exists a sequence $\{w_j\}$ in $C^\infty \cap H^1(\Omega)$ such that

$$(2.15) \quad Trw_j = Trw \quad \text{on } \partial\Omega,$$

$$(2.16) \quad w_j \rightarrow w \quad \text{in } L^2(\Omega),$$

and

$$(2.17) \quad \lim_{j \rightarrow \infty} \Phi_g(w_j) = \Phi_g(w).$$

Therefore, for each $\delta > 0$ there exists a function $\tilde{w}_\delta \in C^\infty \cap H^1(\Omega)$ such that (2.10) and (2.11) hold.

Now suppose also that $Trw = TrG$ on $\partial\Omega$. Then by (2.15), $\tilde{w}_\delta - G \in W_0^{1,1}(\Omega)$, and thus there exists a function $h_\delta \in C_c^\infty(\Omega)$ such that

$$(2.18) \quad \|\tilde{w}_\delta - G - h_\delta\|_{W^{1,1}(\Omega)} + \|\tilde{w}_\delta - G - h_\delta\|_{L^2(\Omega)} \leq \delta.$$

Let $w_\delta = G + h_\delta \in H^1(\Omega)$. Then we have that

$$\begin{aligned} Trw_\delta &= Trw \quad \text{on } \partial\Omega, \\ w_\delta &\rightarrow w \quad \text{in } L^2(\Omega) \quad \text{as } \delta \rightarrow 0, \end{aligned}$$

and

$$\Phi_{\lambda,g}(w_\delta) \leq \Phi_{\lambda,g}(w) + \delta.$$

The proof is complete. \square

Remark 2.5. If $w \in BV \cap L^\infty(\Omega)$, then there exist $w_\delta \in H^1 \cap L^\infty(\Omega)$ such that, in addition to (2.12)–(2.14), we also have that

$$(2.19) \quad \|w_\delta\|_{L^\infty(\Omega)} \leq C(\Omega) \|w\|_{L^\infty(\Omega)}.$$

3. The minimization problem. In this section we study the existence and uniqueness of the solution to minimization problem (1.6). In general, as discussed in [23, 25, 37], there may not exist a minimizer of $\Phi_\lambda(v)$ (see (2.1)), since the limit of the minimizing sequence may not take the boundary value g . However, we can prove the existence of a unique minimizer for a weaker form of (1.6), where we consider the minimization problem using the *relaxed energy*, $\Phi_{\lambda,g}(v)$, defined in (2.3). To this end, we define a pseudosolution of (1.6) as follows.

DEFINITION 3.1. A function $u \in BV \cap L^2(\Omega)$ is a pseudosolution of (1.6) if it is a solution of

$$(3.1) \quad \min_{v \in BV \cap L^2(\Omega)} \Phi_{\lambda,g}(v),$$

where $\Phi_{\lambda,g}(v)$ is defined in (2.3).

First, we show that there exists a pseudosolution of (1.6), that is, a solution of (3.1), in Theorem 3.2. In Theorem 3.5 we provide the motivation for using the notion of pseudosolution in Definition 3.1.

THEOREM 3.2. Suppose $I \in BV \cap L^2(\Omega)$, $g = TrG$ for some function $G \in BV(\Omega)$ with $I = g$ on $\partial\Omega$, and Ω is an open bounded subset of \mathbb{R}^n with Lipschitz boundary. Then there exists a unique pseudosolution of (1.6) as given in Definition 3.1.

Proof. Let $\{u_n\}$ be a minimizing sequence of (3.1) in $BV \cap L^2(\Omega)$. Since $\{u_n\}$ is bounded in $BV(\Omega)$ and $L^2(\Omega)$, using the compactness of $BV(\Omega)$ and the weak compactness of $L^2(\Omega)$, we see that there exists a subsequence $\{u_{n_k}\}$ of $\{u_n\}$ and a function $u \in BV \cap L^2(\Omega)$ satisfying

$$(3.2) \quad u_{n_k} \rightarrow u \quad \text{strongly in } L^1(\Omega),$$

$$(3.3) \quad u_{n_k} \rightharpoonup u \quad \text{weakly in } L^2(\Omega).$$

By (3.2), (3.3), Lemma 2.3, and the weak lower semicontinuity of the L^2 -norm, we have that

$$\Phi_{\lambda,g}(u) \leq \liminf_{k \rightarrow \infty} \Phi_{\lambda,g}(u_{n_k}) = \inf_{BV \cap L^2(\Omega)} \Phi_{\lambda,g}(v).$$

Hence, u is a solution of the minimization problem. Uniqueness follows from the strict convexity of $\Phi_{\lambda,g}(v)$ in v . \square

To better understand the relationship between (1.6) and (3.1), we need the following two lemmas. For $\beta > 0$, let

$$(3.4) \quad d_\beta(x) = \min\left(\frac{d(x)}{\beta}, 1\right),$$

where $d(x)$ is the distance of the point x to the boundary of Ω .

LEMMA 3.3 (*Theorem A.1 of [19]*). *For each $v \in BV \cap L^\infty(\Omega)$, the vector measures $v\nabla d_\beta$ converge weakly to $-v\gamma d\mathcal{H}^{n-1}$ as $\beta \rightarrow 0$, where γ is the unit outward normal to $\partial\Omega$, and*

$$\lim_{\beta \rightarrow 0} \int_{\Omega} |v| |\nabla d_\beta| = \int_{\partial\Omega} |v| d\mathcal{H}^{n-1}.$$

LEMMA 3.4. *Let $G \in W^{1,1} \cap L^\infty(\Omega)$. Then for any $v \in BV \cap L^\infty(\Omega)$, there exists a sequence $\{v_\beta\}$ in $BV \cap L^\infty(\Omega)$ such that*

$$\begin{aligned} Tr v_\beta &= Tr G \quad \text{in } L^1(\partial\Omega), \\ v_\beta &\rightarrow v \quad \text{in } L^2(\Omega) \quad \text{as } \beta \rightarrow 0, \end{aligned}$$

and

$$\lim_{\beta \rightarrow 0} \Phi_g(v_\beta) = \Phi_g(v).$$

Proof. For $\beta > 0$, define $d_\beta(x)$ as in (3.4). Since $d(x) \in W^{1,\infty}(\Omega)$ and $|\nabla d| = 1$, we have that

$$(3.5) \quad |\nabla d_\beta| = \frac{1}{\beta} \text{ if } d(x) < \beta \quad \text{and} \quad |\nabla d_\beta| = 0 \text{ if } d(x) \geq \beta.$$

Fix $v \in BV \cap L^\infty(\Omega)$ and let $v_\beta = d_\beta v + (1 - d_\beta)G$ for $(x, t) \in \Omega$. Then

$$\begin{aligned} v_\beta &\in BV \cap L^\infty(\Omega) \text{ with } Tr v_\beta = Tr G \text{ in } L^1(\partial\Omega), \\ v_\beta &\rightarrow v \text{ in } L^2(\Omega). \end{aligned}$$

By Lemma 2.3, $\liminf_{\beta \rightarrow 0} \Phi_g(v_\beta) \geq \Phi_g(v)$, and thus it remains only to show that

$$(3.6) \quad \lim_{\beta \rightarrow 0} \Phi_g(v_\beta) \leq \Phi_g(v).$$

Writing $\Phi_g = \tilde{\Phi}_g$ (Lemma 2.3), since $D^s v_\beta = d_\beta D^s v$ and $Tr v_\beta = Tr G$ in $L^1(\partial\Omega)$ we have that

$$\begin{aligned} \tilde{\Phi}_g(v_\beta) &= \sup_{\substack{\psi \in C^1(\overline{\Omega}, \mathbb{R}^n) \\ |\psi| \leq 1}} \left[\int_{\Omega} \{(v - G)\nabla d_\beta + d_\beta \nabla v + (1 - d_\beta)\nabla G\} \cdot \psi \right. \\ &\quad \left. - \frac{q(x) - 1}{q(x)} |\psi|^{\frac{q(x)}{q(x)-1}} dx + \int_{\Omega} d_\beta D^s v \cdot \psi \right]. \end{aligned}$$

Therefore, by (2.5)

$$\begin{aligned}\tilde{\Phi}(v_\beta) &\leq \sup_{\substack{\psi \in C^1(\bar{\Omega}, \mathbb{R}^n) \\ |\psi| \leq 1}} \left[\int_{\Omega} \nabla v \cdot \psi - \frac{q(x)-1}{q(x)} |\psi|^{\frac{q(x)}{q(x)-1}} dx \right] \\ &\quad + \int_{\Omega} |v - G| |\nabla d_\beta| dx + \int_{\Omega} (1 - d_\beta)(|\nabla v| + |\nabla G|) dx + \int_{\Omega} d_\beta |D^s v| \\ &= \int_{\Omega} \phi(x, \nabla v) + \int_{\Omega} |v - G| |\nabla d_\beta| dx + \int_{\Omega} (1 - d_\beta)(|\nabla v| + |\nabla G|) dx + \int_{\Omega} d_\beta |D^s v|.\end{aligned}$$

By Lemma 3.3, as $\beta \rightarrow 0$,

$$\int_{\Omega} |v - G| |\nabla d_\beta| dx \rightarrow \int_{\partial\Omega} |v - G| d\mathcal{H}^{n-1}.$$

Furthermore, the Lebesgue dominated convergence theorem gives us that

$$\int_{\Omega} (1 - d_\beta)(|\nabla v| + |\nabla G|) dx \rightarrow 0 \quad \text{and} \quad \int_{\Omega} d_\beta |D^s v| \rightarrow \int_{\Omega} |D^s v|.$$

Therefore, (3.6) holds and the lemma is proved. \square

THEOREM 3.5. *We have that*

$$(3.7) \quad \inf_{v \in BV_g \cap L^2(\Omega)} \Phi_\lambda(v) = \min_{v \in BV \cap L^2(\Omega)} \Phi_{\lambda,g}(v),$$

where Φ_λ and $\Phi_{\lambda,g}$ are as defined in (2.1) and (2.3), respectively, and BV_g is as defined in (1.7).

Proof. Since $BV_g(\Omega) \subset BV(\Omega)$,

$$\inf_{v \in BV \cap L^2(\Omega)} \Phi_{\lambda,g}(v) \leq \inf_{v \in BV_g \cap L^2(\Omega)} \Phi_{\lambda,g}(v) = \inf_{v \in BV_g \cap L^2(\Omega)} \Phi_\lambda(v).$$

To see the reverse, let $u \in BV \cap L^2(\Omega)$ be the solution of (3.1). By Lemma 3.4, there exist $v_\beta \in BV_g \cap L^\infty(\Omega)$ such that

$$\Phi_\lambda(v_\beta) = \Phi_{\lambda,g}(v_\beta) \xrightarrow{\beta \rightarrow 0} \Phi_{\lambda,g}(u) = \min_{v \in BV \cap L^2(\Omega)} \Phi_{\lambda,g}(v),$$

and thus

$$\inf_{v \in BV_g \cap L^2(\Omega)} \Phi_\lambda(v) \leq \min_{v \in BV \cap L^2(\Omega)} \Phi_{\lambda,g}(v).$$

Thus, the theorem holds. \square

4. The flow related to minimization problem (3.1).

4.1. Motivation for the weak solution. Due to the boundary term, the lower semicontinuity of $\Phi_{\lambda,g}$ with respect to the L^2 -norm is not clear. Therefore, the notion of solution using the theory of maximal monotone operators [12] cannot be directly applied. However, we can establish the existence and uniqueness of the solution in the following sense. Suppose that

$$(4.1) \quad v \in L^2(0, T; H^1(\Omega))$$

and that u is a classical solution of (1.8)–(1.10). Multiplying (1.8) by $(v - u)$, integrating over Ω , and using the convexity of ϕ , we have that

$$(4.2) \quad \int_{\Omega} \dot{u}(v - u) dx + \Phi_{\lambda,g}(v) \geq \Phi_{\lambda,g}(u).$$

Integrating over $[0, s]$ for any $s \in [0, T]$ then yields

$$(4.3) \quad \int_0^s \int_{\Omega} \dot{u}(v - u) dx dt + \int_0^s \Phi_{\lambda,g}(v) dt \geq \int_0^s \Phi_{\lambda,g}(u) dt.$$

On the other hand, setting $v = u + \epsilon w$ in (4.3) with $w \in C_0^\infty(\Omega)$ makes it clear that

$$\int_0^s \int_{\Omega} \dot{u}(\epsilon w) dx dt + \int_0^s \Phi_{\lambda,g}(u + \epsilon w) dt$$

attains a minimum at $\epsilon = 0$. Therefore, if u satisfies (4.3) and $u \in L^2(0, T; BV \cap L^2(\Omega))$ with $\dot{u} \in L^2(\Omega^T)$, u is also a solution of (1.8)–(1.10) in the sense of distribution. This motivates the following definition.

DEFINITION 4.1. *We say that a function $u \in L^2(0, T; BV \cap L^2(\Omega))$ with $\dot{u} \in L^2(\Omega^T)$ is a pseudosolution of (1.8)–(1.10) if*

1. $u(x, 0) = I(x)$ on Ω , and
2. u satisfies (4.3) for all $s \in [0, T]$ and $v \in L^2(0, T; BV \cap L^2(\Omega))$.

4.2. The approximate functional ϕ^ϵ .

For $\epsilon > 0$, define

$$(4.4) \quad \phi^\epsilon(x, r) := \begin{cases} \frac{1}{q(x)} |r|^{q(x)}, & |r| \leq 1, \\ \frac{1}{1+\epsilon} |r|^{(1+\epsilon)} - \frac{q(x)-(1+\epsilon)}{(1+\epsilon)q(x)}, & |r| > 1. \end{cases}$$

Remark 4.2. We note the following properties, as they will be useful in later computations:

1. $\phi^\epsilon(x, r)$ is convex in r .
2. $\phi_r^\epsilon(x, r) \cdot r \geq 0$ for all $r \in \mathbb{R}^n$.
3. $\phi(x, r) \leq \phi^\epsilon(x, r)$ for all $r \in \mathbb{R}^n$.

To prove the existence and uniqueness of the pseudosolution of (1.8)–(1.10), we first study solutions of the approximate problem

$$(4.5) \quad \dot{u} - \epsilon \Delta u - \operatorname{div}(\phi_r^\epsilon(x, \nabla u)) + \lambda(u - I) = 0 \quad \text{in } \Omega \times [0, T],$$

$$(4.6) \quad u(x, t) = g(x) \quad \text{in } \partial\Omega \times [0, T],$$

$$(4.7) \quad u(x, 0) = \tilde{I}(x) \quad \text{in } \Omega,$$

where $\tilde{I} \in H^1 \cap L^\infty(\Omega)$, $g \in L^\infty(\partial\Omega)$ with $g = TrG$ on $\partial\Omega$ for some $G \in H^1(\Omega)$, and $\tilde{I}|_{\partial\Omega} = g$.

LEMMA 4.3. *Suppose $\tilde{I} \in H^1(\Omega)$ with $\tilde{I}|_{\partial\Omega} = g$. Then problem (4.5)–(4.7) has a unique solution $u \in L^2(0, T; H^1(\Omega)) \cap C(0, T; L^2(\Omega))$ with $\dot{u} \in L^2(0, T; L^2(\Omega))$ such that*

$$(4.8) \quad \begin{aligned} \int_0^\infty \int_{\Omega} |\dot{u}|^2 dx dt + \sup_{t>0} \left[\int_{\Omega} \frac{\epsilon}{2} |\nabla u|^2 + \phi^\epsilon(x, \nabla u) + \frac{\lambda}{2} |u - \tilde{I}|^2 \right] \\ \leq \int_{\Omega} \frac{\epsilon}{2} |\nabla \tilde{I}|^2 + \phi^\epsilon(x, \nabla \tilde{I}) dx. \end{aligned}$$

Proof. Since (4.5) is uniformly parabolic, we can conclude this lemma by standard results for parabolic equations [24] and the corresponding energy estimate. \square

4.3. Estimates for the solution of the approximate problem.

LEMMA 4.4. *If $\tilde{I} \in H^1 \cap L^\infty \cap BV(\Omega)$, $g \in L^\infty(\partial\Omega)$ with $\tilde{I}|_{\partial\Omega} = g$, and u is a solution of (4.5)–(4.7), then*

$$(4.9) \quad \|u\|_{L^\infty(\Omega^T)} \leq \max(\|\tilde{I}\|_{L^\infty(\Omega)}, \|g\|_{L^\infty(\partial\Omega)}).$$

Proof. Let $M := \max(\|\tilde{I}\|_{L^\infty(\Omega)}, \|g\|_{L^\infty(\partial\Omega)})$. Multiply (4.5) by $(u - M)_+$, where

$$(u - M)_+ = \begin{cases} u - M & \text{if } u - M \geq 0, \\ 0 & \text{otherwise,} \end{cases}$$

and integrate over Ω to get

$$(4.10) \quad \int_{\Omega} \dot{u}(u - M)_+ dx + \epsilon \int_{\Omega} |\nabla u|^2 dx + \int_{\Omega} \phi_r^\epsilon(x, \nabla u) \cdot \nabla u dx + \lambda \int_{\Omega} (u - \tilde{I})(u - M)_+ dx = 0.$$

By property 2 of Remark 4.2, we have that $\int_{\Omega} \phi_r^\epsilon(x, \nabla u) \cdot \nabla u dx \geq 0$, and thus

$$\frac{1}{2} \int_{\Omega} \frac{d}{dt} (u - M)_+^2 dx \leq 0.$$

Therefore, $\frac{1}{2} \int_{\Omega} (u - M)_+^2 dx$ is decreasing in t , and since

$$\frac{1}{2} \int_{\Omega} (u - M)_+^2 dx \geq 0 \quad \text{and} \quad \frac{1}{2} \int_{\Omega} (u - M)_+^2 dx|_{t=0} = 0,$$

we have that

$$\frac{1}{2} \int_{\Omega} (u - M)_+^2 dx = 0 \quad \text{for all } t \in [0, T],$$

and thus

$$u(t) \leq M = \max(\|\tilde{I}\|_{L^\infty(\Omega)}, \|g\|_{L^\infty(\partial\Omega)}) \text{ } \mathcal{L}\text{-a.e. on } \Omega \text{ for all } t > 0.$$

Multiplying (4.5) by $(u + M)_+$, a similar argument yields that $u(t) \geq -M$ for all t . Equation (4.9) follows directly. \square

LEMMA 4.5. *Let u be the solution of (4.5)–(4.7). Then for all $v \in L^2(0, T; H^1(\Omega))$ with $v|_{\partial\Omega} = g$,*

$$(4.11) \quad \begin{aligned} & \int_0^s \int_{\Omega} \dot{u}(v - u) + \frac{\epsilon}{2} |\nabla v|^2 + \phi^\epsilon(x, Dv) + \frac{\lambda}{2} |v - \tilde{I}|^2 dx dt \\ & \geq \int_0^s \int_{\Omega} \frac{\epsilon}{2} |\nabla u|^2 + \phi^\epsilon(x, Du) + \frac{\lambda}{2} |u - \tilde{I}|^2 dx dt. \end{aligned}$$

Proof. Multiplying (4.5) by $v - u$, then integrating by parts and using the convexity of $\phi^\epsilon(x, r)$ in r , we see that (4.11) follows. \square

Remark 4.6. Let u be the solution of (4.5)–(4.7). Then for any $0 < \epsilon < \alpha - 1$ (where $1 < \alpha \leq q(x)$), we have the following estimate, which is a direct consequence of Lemma 4.3:

$$(4.12) \quad \int_0^\infty \int_{\Omega} |\dot{u}|^2 dx dt + \sup_{t>0} \left[\int_{\Omega} \frac{1}{1+\epsilon} |\nabla u|^{1+\epsilon} dx + \frac{\lambda}{2} \int_{\Omega} |u - \tilde{I}|^2 dx \right] \leq C,$$

where $C > 0$ is a constant depending only on Ω and $\|\nabla \tilde{I}\|_{L^2(\Omega)}$.

4.4. Existence and uniqueness of (1.8)–(1.10). Suppose I is given as in Theorem 3.2. By Lemma 2.4 and Remark 2.5, there exists a sequence $\{I_\delta\}$ in $H^1 \cap L^\infty(\Omega)$ such that

$$(4.13) \quad Tr I_\delta = Tr I \quad \text{on } \partial\Omega,$$

$$(4.14) \quad \|I_\delta\|_{L^\infty(\Omega)} \leq C \|I\|_{L^\infty(\Omega)},$$

$$(4.15) \quad I_\delta \rightarrow I \quad \text{strongly in } L^2(\Omega) \quad \text{as } \delta \rightarrow 0,$$

and

$$(4.16) \quad \Phi_{\lambda,g}(I_\delta) \leq \Phi_{\lambda,g}(I) + \delta.$$

THEOREM 4.7 (existence and uniqueness). Suppose $I \in BV \cap L^\infty(\Omega)$, $g \in L^\infty(\partial\Omega)$, and $I|_{\partial\Omega} = g$ with $g = Tr G$ for some function $G \in H^1(\Omega)$. Then there exists a unique pseudosolution u of (1.8)–(1.10) in the sense of Definition 4.1.

Proof. Step 1. First, we fix $\delta > 0$ and pass to the limit $\epsilon \rightarrow 0$.

Let $\{u_\delta^\epsilon\}$ be the sequence of solutions to (4.5)–(4.7) with initial data $\tilde{I} = I_\delta$. By Lemma 4.4 and Remark 4.6, there exists a subsequence $\{u_\delta^{\epsilon_i}\}$ and a function $u_\delta \in L^\infty(\Omega^\infty)$ with $\dot{u}_\delta \in L^2(\Omega^\infty)$ such that as $\epsilon_i \rightarrow 0$,

$$(4.17) \quad u_\delta^{\epsilon_i} \rightharpoonup u_\delta \quad \text{weakly}^* \text{ in } L^\infty(\Omega^\infty),$$

$$(4.18) \quad \dot{u}_\delta^{\epsilon_i} \rightharpoonup w \quad \text{weakly in } L^2(\Omega^\infty).$$

The same argument used in the proof of Lemma 3.1 in [37] gives us that $\dot{u}_\delta = w$ and $u_\delta(0) = I_\delta$.

Moreover, for all $f \in L^2(\Omega)$,

$$\begin{aligned} \int_{\Omega} (u_\delta^{\epsilon_i}(\cdot, t) - I_\delta) f(x) dx &= \int_0^\infty \int_{\Omega} \dot{u}_\delta^{\epsilon_i}(x, s) 1_{[0,t]}(s) f(x) dx ds \\ &\xrightarrow{\epsilon_i \rightarrow 0} \int_0^\infty \int_{\Omega} \dot{u}_\delta(x, s) 1_{[0,t]}(s) f(x) dx ds \\ &= \int_{\Omega} (u_\delta(\cdot, t) - I_\delta) f(x) dx. \end{aligned}$$

Therefore, for each $t > 0$,

$$(4.19) \quad u_\delta^{\epsilon_i}(\cdot, t) \rightharpoonup u_\delta(\cdot, t) \quad \text{weakly in } L^2(\Omega).$$

From (4.12), for each $t > 0$, $\{u_\delta^{\epsilon_i}\}$ is a bounded sequence in $W^{1,1}(\Omega)$. Therefore, there exists a convergent subsequence $\{u_\delta^{\epsilon_{i_j}}\}$ of $\{u_\delta^{\epsilon_i}\}$ such that

$$u_\delta^{\epsilon_{i_j}}(\cdot, t) \rightarrow u_\delta(\cdot, t) \quad \text{strongly in } L^1(\Omega).$$

Note that every convergent subsequence of $\{u_\delta^{\epsilon_i}\}$ converges to the same limit $u_\delta(\cdot, t)$ due to (4.19). Then, for each $t > 0$,

$$(4.20) \quad u_\delta^{\epsilon_i}(\cdot, t) \rightarrow u_\delta(\cdot, t) \quad \text{strongly in } L^1(\Omega).$$

From (4.17) and (4.20), we have that for each $t > 0$,

$$(4.21) \quad u_\delta^{\epsilon_i}(\cdot, t) \rightarrow u_\delta(\cdot, t) \quad \text{strongly in } L^2(\Omega).$$

We also have from (4.12) and (4.20) that $u_\delta \in L^\infty(0, \infty; BV \cap L^\infty(\Omega))$ with $\dot{u}_\delta \in L^2(\Omega^\infty)$. Furthermore, by Lemma 4.5, for all $v \in L^2(0, T; H^1(\Omega))$ with $v|_{\partial\Omega} = g$,

$$(4.22) \quad \begin{aligned} & \int_0^s \int_\Omega \dot{u}_\delta^{\epsilon_i}(v - u_\delta^{\epsilon_i}) + \frac{\epsilon_i}{2} |\nabla v|^2 + \phi^{\epsilon_i}(x, \nabla v) + \frac{\lambda}{2} |v - I_\delta|^2 dx dt \\ & \geq \int_0^s \int_\Omega \frac{\epsilon_i}{2} |\nabla u_\delta^{\epsilon_i}|^2 + \phi^{\epsilon_i}(x, Du_\delta^{\epsilon_i}) + \frac{\lambda}{2} |u_\delta^{\epsilon_i} - I_\delta|^2 dx dt. \end{aligned}$$

Using (4.18) and (4.21), we can let $\epsilon_i \rightarrow 0$ in (4.22) to get

$$(4.23) \quad \begin{aligned} & \int_0^s \int_\Omega \dot{u}_\delta(v - u_\delta) + \phi(x, \nabla v) + \frac{\lambda}{2} |v - I_\delta|^2 dx dt \\ & \geq \lim_{\epsilon_i \rightarrow 0} \int_0^s \int_\Omega \phi^{\epsilon_i}(x, Du_\delta^{\epsilon_i}) dx dt + \frac{\lambda}{2} \int_0^s \int_\Omega |u_\delta - I_\delta|^2 dx dt. \end{aligned}$$

By Lemma 2.3, weak lower semicontinuity (w.l.s.c.), and property 3 of Remark 4.2,

$$(4.24) \quad \lim_{\epsilon_i \rightarrow 0} \int_0^s \int_\Omega \phi^{\epsilon_i}(x, Du_\delta^{\epsilon_i}) dx dt \geq \int_0^s \int_\Omega \phi(x, Du_\delta) dx dt + \int_0^s \int_{\partial\Omega} |u_\delta - g| d\mathcal{H}^{n-1} dt.$$

The combination of (4.23) and (4.24) gives us

$$(4.25) \quad \begin{aligned} & \int_0^s \int_\Omega \dot{u}_\delta(v - u_\delta) + \phi(x, \nabla v) + \frac{\lambda}{2} |v - I_\delta|^2 dx dt + \int_0^s \int_{\partial\Omega} |v - g| d\mathcal{H}^{n-1} dt \\ & \geq \int_0^s \int_\Omega \phi(x, \nabla u_\delta) + \frac{\lambda}{2} |u_\delta - I_\delta|^2 dx dt + \int_0^s \int_{\partial\Omega} |u_\delta - g| d\mathcal{H}^{n-1} dt \end{aligned}$$

for all $v \in L^2(0, \infty; H^1(\Omega))$ with $v = g$ on $\partial\Omega^\infty$. By approximation, (4.25) still holds for $v \in L^2(0, \infty; BV \cap L^\infty(\Omega))$ with $v = g$ on $\partial\Omega^\infty$. To see that (4.25) holds for all $v \in L^2(0, \infty; BV \cap L^\infty(\Omega))$ (in particular, without $v = g$ on $\partial\Omega^\infty$), replace v with $v_\beta = d_\beta v + (1 - d_\beta)G$ in (4.25) and (by Lemma 3.4) let $\beta \rightarrow 0$. By approximation, we can conclude that (4.25) holds for all $v \in L^2(0, \infty; BV \cap L^2(\Omega))$.

Step 2. Now it remains only to pass to the limit as $\delta \rightarrow 0$ in (4.25) to complete the proof. First note that (4.8) holds for $u_\delta^{\epsilon_i}$ with $\tilde{I} = I_\delta$. Fix $\delta > 0$. By w.l.s.c. and (4.20), the same argument used to deduce (4.24) also gives us that

$$\lim_{\epsilon_i \rightarrow 0} \int_\Omega \phi^{\epsilon_i}(x, Du_\delta^{\epsilon_i}) dx \geq \int_\Omega \phi(x, Du_\delta) dx + \int_{\partial\Omega} |u_\delta - g| d\mathcal{H}^{n-1}.$$

Therefore, we can pass to the limit as $\epsilon_i \rightarrow 0$ in (4.8) and get

$$(4.26) \quad \begin{aligned} & \int_0^\infty \int_\Omega |\dot{u}_\delta|^2 dx dt + \sup_{t>0} \left[\int_\Omega \phi(x, Du_\delta) dx dt + \frac{\lambda}{2} |u_\delta - I_\delta|^2 + \int_{\partial\Omega} |u_\delta - g| d\mathcal{H}^{n-1} dt \right] \\ & \leq \int_\Omega \phi(x, \nabla I_\delta) dx. \end{aligned}$$

Then $\{u_\delta\}$ is uniformly bounded in $W^{1,1}(\Omega)$ for each $t > 0$. Note also that in Lemma 4.4 the bound is independent of both ϵ and δ . Therefore, $\{u_\delta\}$ is also uniformly bounded in $L^\infty(\Omega^\infty)$. From (4.26), we also have that $\{\dot{u}_\delta\}$ is uniformly bounded in $L^2(\Omega^\infty)$.

By the same argument used to obtain (4.17), (4.18), and (4.21), there exists a subsequence $\{u_{\delta_j}\}$ of $\{u_\delta\}$ and a function $u \in L^\infty(0, \infty; BV \cap L^\infty(\Omega))$ with $\dot{u} \in L^2(\Omega^\infty)$ such that as $\delta_j \rightarrow 0$,

$$(4.27) \quad u_{\delta_j} \rightharpoonup u \quad \text{weakly}^* \text{ in } L^\infty(\Omega^\infty),$$

$$(4.28) \quad \dot{u}_{\delta_j} \rightharpoonup \dot{u} \quad \text{weakly in } L^2(\Omega^\infty),$$

$$(4.29) \quad u_{\delta_j}(\cdot, t) \rightarrow u(\cdot, t) \quad \text{strongly in } L^2(\Omega) \text{ and uniformly in } t.$$

Let $\delta = \delta_j$ in (4.25). Using w.l.s.c. and (4.27)–(4.29), we can let $\delta_j \rightarrow 0$ in (4.25) to conclude that for all $v \in L^2(0, \infty; BV \cap L^2(\Omega))$,

$$\int_0^s \int_\Omega \dot{u}(v - u) dx dt + \int_0^s \Phi_{\lambda, g}(v) dt \geq \int_0^s \Phi_{\lambda, g}(u) dt.$$

Existence is proved.

Step 3 (uniqueness). Suppose that u_1, u_2 are both weak solutions of (1.8)–(1.10). As in [23, 37], we can obtain two inequalities: the first by setting $u = u_1$ and $v = u_2$ in (4.3) and the second by setting $u = u_2$ and $v = u_1$. Adding these two inequalities gives us that for all $s > 0$,

$$\int_0^s \int_\Omega \frac{1}{2} \frac{d}{dt} |u_1 - u_2|^2 dx dt \leq 0.$$

Therefore, $u_1 = u_2$ in Ω^∞ . \square

4.5. Behavior as $t \rightarrow \infty$.

THEOREM 4.8. *As $t \rightarrow \infty$, the weak solution, $u(x, t)$, of (1.8)–(1.10) converges strongly in $L^2(\Omega)$ to a minimizer \tilde{u} of the function $\Phi_{\lambda, g}$, i.e., the pseudosolution, \tilde{u} , of (3.1).*

Proof. Since u satisfies (4.3), for any $s > 0$ we can substitute $v(x) \in BV \cap L^2(\Omega)$ into (4.3) as follows:

$$(4.30) \quad \begin{aligned} & \int_\Omega (u(x, s) - I(x)) v(x) dx - \frac{1}{2} \int_\Omega (u^2(x, s) - I^2(x)) dx + s \int_\Omega \phi(x, \nabla v) \\ & + s \frac{\lambda}{2} \int_\Omega |v - I|^2 dx + s \int_{\partial\Omega} |v - g| d\mathcal{H}^{n-1} \\ & \geq \int_0^s \int_\Omega \phi(x, \nabla u) dt + \frac{\lambda}{2} \int_0^s \int_\Omega |u - I|^2 dx dt + \int_0^s \int_{\partial\Omega} |u - g| d\mathcal{H}^{n-1} dt. \end{aligned}$$

Proceeding as in [19], let

$$w(x, s) = \frac{1}{s} \int_0^s u(x, t) dt.$$

Since $u \in L^\infty(0, \infty; BV \cap L^\infty(\Omega))$, for each $s > 0$ we have that $w(\cdot, s) \in BV \cap L^\infty(\Omega)$ with $\{w(\cdot, s)\}$ uniformly bounded in $BV(\Omega)$ and $L^\infty(\Omega)$. Therefore, there exists a subsequence $\{w(\cdot, s_i)\}$ of $\{w(\cdot, s)\}$ which converges strongly in $L^1(\Omega)$ and weakly in $BV(\Omega)$ and $L^\infty(\Omega)$ to a function $\tilde{u} \in BV \cap L^\infty(\Omega)$ as $s_i \rightarrow \infty$. Since $\{w(\cdot, s)\}$ is uniformly bounded in $L^\infty(\Omega)$, $\{w(\cdot, s_i)\}$ also converges strongly in $L^2(\Omega)$ to \tilde{u} .

Dividing (4.30) by s and taking the limit along $s_i \rightarrow \infty$ gives us that

$$\begin{aligned} \int_{\Omega} \phi(x, \nabla v) + \frac{\lambda}{2} \int_{\Omega} |v - I|^2 dx + \int_{\partial\Omega} |v - g| d\mathcal{H}^{n-1} &\geq \int_{\Omega} \phi(x, \nabla \tilde{u}) \\ &+ \frac{\lambda}{2} \int_{\Omega} |\tilde{u} - I|^2 dx + \int_{\partial\Omega} |\tilde{u} - g| d\mathcal{H}^{n-1} \end{aligned}$$

for all $v \in BV \cap L^2(\Omega)$; i.e., \tilde{u} is a pseudosolution of (3.1). \square

5. Numerical methods and experimental results. We solve the minimization problem (1.3) numerically using the flow of its associated Euler–Lagrange equation,

$$(5.1) \quad \frac{\partial u}{\partial t} - \operatorname{div}(\phi_r(x, Du)) + \lambda(u - I) = 0 \quad \text{in } \Omega \times [0, T],$$

$$(5.2) \quad \frac{\partial u}{\partial n}(x, t) = 0 \quad \text{on } \partial\Omega \times [0, T],$$

$$(5.3) \quad u(0) = I \quad \text{in } \Omega.$$

To approximate (5.1), we use an explicit finite difference scheme. The degenerate diffusion term,

$$\begin{aligned} &\operatorname{div}(\phi_r(x, \nabla u)) \\ &= |\nabla u|^{p(x)-2} \left[(p(x) - 1)\Delta u + (2 - p(x))|\nabla u|\operatorname{div}\left(\frac{\nabla u}{|\nabla u|}\right) + \nabla p \cdot \nabla u \log|\nabla u| \right] \end{aligned}$$

with

$$(5.4) \quad p(x) = \begin{cases} q(x) \equiv 1 + \frac{1}{1+k|\nabla G_{\sigma}*I(x)|^2}, & |\nabla u| < \beta, \\ 1, & |\nabla u| \geq \beta \end{cases}$$

for $k, \sigma > 0$, and G_{σ} the Gaussian filter, is approximated as follows:

- The coefficient, $|\nabla u|^{p(x)-2}$, is approximated using central differences;
- the isotropic diffusion term, Δu , is approximated using central differences;
- the curvature term, $|\nabla u|\operatorname{div}\left(\frac{\nabla u}{|\nabla u|}\right)$, is approximated using the minmod scheme for $\operatorname{div}\left(\frac{\nabla u}{|\nabla u|}\right)$ (see [31]) and central differences for $|\nabla u|$;
- if $|\nabla u| \neq 0$, the hyperbolic term $\nabla p \cdot \nabla u \log|\nabla u|$ is computed using an upwind scheme for $\nabla p \cdot \nabla u$ (see [29]) and central differences for $\log|\nabla u|$. Otherwise, the hyperbolic term is set to zero.

We found that the behavior of (1.3) is an innate behavior of the model, and variants on this numerical scheme also yield very good results.

We compared our model with the flow of the Euler–Lagrange equation associated with (1.2) (modified only by a fidelity term),

$$(5.5) \quad \frac{\partial u}{\partial t} = (p - 1)\Delta u + (2 - p)\operatorname{div}\left(\frac{\nabla u}{|\nabla u|}\right) - \lambda(u - I), \quad \text{where } p = \begin{cases} 2, & |\nabla u| < \beta, \\ 1, & |\nabla u| \geq \beta. \end{cases}$$

An explicit finite difference scheme was used, where central differences were used to implement Δu and the minmod scheme [31] was used to implement $\text{div}(\frac{\nabla u}{|\nabla u|})$.

All of the images ranged in intensity from 0 to 255. The parameters $\lambda = .05$, $\sigma = .5$, $k = .0075$ and time step = .05 consistently yielded optimal results for all of the models we tested here. We compared various thresholds, β , to test the sensitivity of both models (1.2) and (1.3) to this parameter. All of the “edge maps” in the figures to follow were computed using the function

$$(5.6) \quad \text{edge map of } u: \frac{1}{1 + k|\nabla G_\sigma * u(x)|^2}$$

with $k = .0075$ (the same value of k is also used to compute the exponent $p(x)$ in (5.4)). We found that this value also gave the clearest edge map for each model. The number of iterations was chosen large enough so that the standard deviation between subsequent images was at most .005.

In Figure 5.1 we illustrate the proposed model’s ability to reconstruct piecewise smooth functions while avoiding the staircasing effect. The first row from the top contains a piecewise smooth function plotted as both an image and a surface, and also contains its edge map (5.6). The surface is viewed from two different orientations: the first view displays the upper left corner of the image at the origin, and the second view displays the same surface rotated 180°. The second row contains the same series of images for the image degraded by Gaussian noise with mean zero. The third, fourth, and fifth rows contain reconstructions using isotropic diffusion only ($p \equiv 2$), TV-based diffusion only ($p \equiv 1$), and the proposed model, respectively. Isotropic diffusion reconstructs smooth regions, but edges are severely blurred. TV-based diffusion reconstructs sharp edges, but the staircasing effect is clearly present. This in turn creates false edges, which could lead to an incorrect segmentation of the image. The proposed model reconstructs sharp edges as effectively as TV-based diffusion and recovers smooth regions as effectively as pure isotropic diffusion (in particular, without staircasing).

Figure 5.2 contains a reconstruction of another piecewise smooth image with additive Gaussian noise. Our goal is to once again reconstruct the smooth regions while preserving their boundaries and without introducing false edges. Furthermore, we also wanted to compare the sensitivity of models (1.2) and (1.3) to the threshold, β . The top row shows the original and noisy images with their edge maps (5.6). The bottom three rows contain reconstructions using models (1.2) and (1.3). The first column from the left contains reconstructions using (1.2) with thresholds $\beta = 30, 50$, and 70, respectively, and the second column contains their corresponding edge maps (5.6). The third column contains reconstructions using TV-based diffusion only ((1.2) or (1.3) with $\beta = 0$) and the proposed model (1.3) with thresholds $\beta = 30$ and 100, respectively. The last column contains their corresponding edge maps (5.6). TV-based diffusion only ($\beta = 0$) shows clear evidence of staircasing, while the proposed model is relatively insensitive to a broad range of thresholds, β . Although the exact behavior of the diffusion changes slightly at likely edges between $\beta = 30$ and $\beta = 100$, the effect on the resulting image is minimal. On the other hand, model (1.2) demonstrates a large change in behavior at both noise and edges across the range of thresholds $\beta = 30, 50$, and 70. Similar experiments on the noisy radar images in Figures 5.3 and 5.4 yielded very similar results. Note that in Figure 5.3, even fine details, such as the lettering at the bottom of the image, are preserved using the proposed model. In Figure 5.4, the proposed model preserves the boundaries of the land mines as effectively as the TV model without enhancing the background noise.

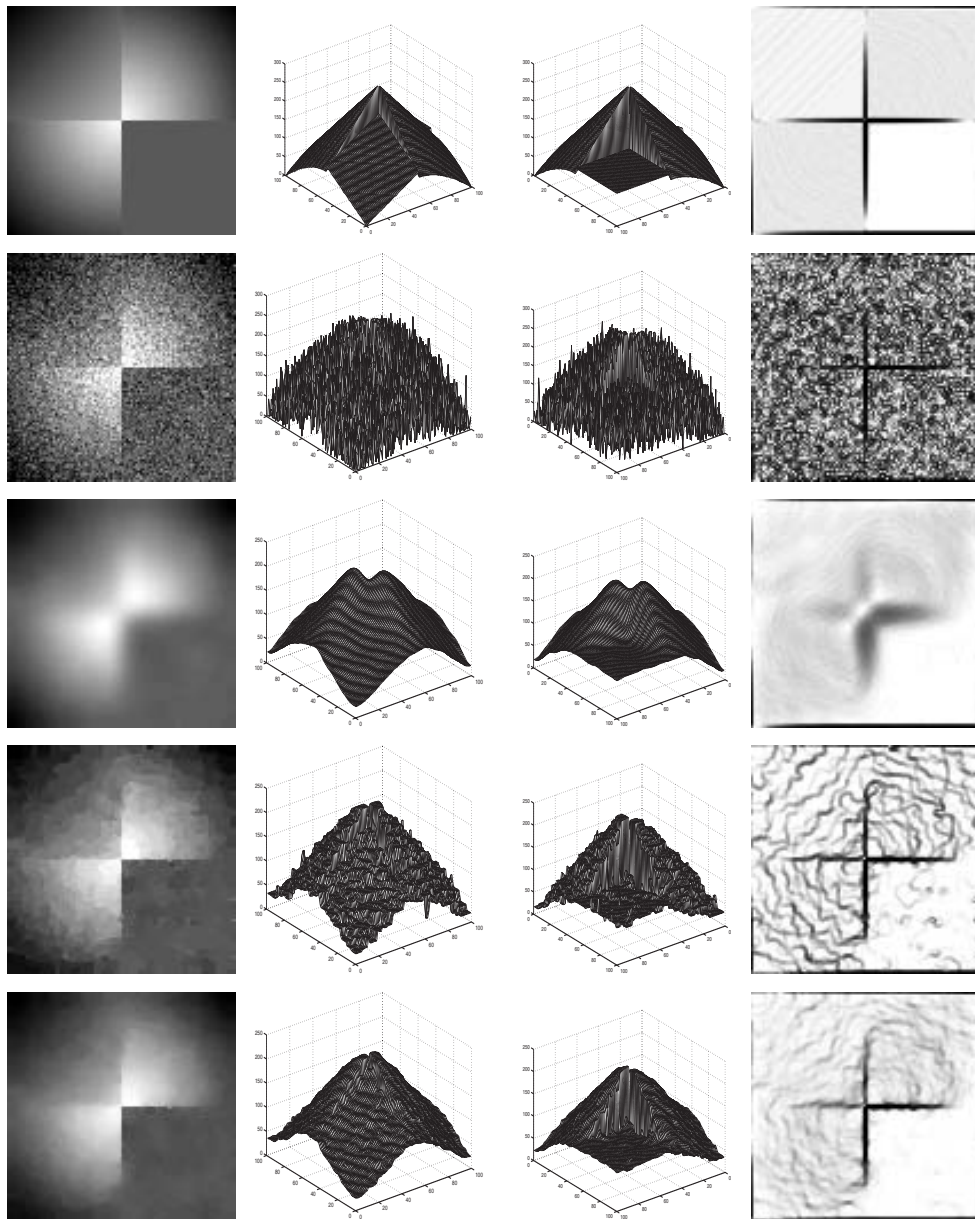


FIG. 5.1. Top row: true image (100×100), surface plot of the image, surface rotated 180° , edge map (5.6). Second row: image + noise. Third row: reconstruction using isotropic diffusion only (200 iterations). Fourth row: reconstruction using TV-based diffusion only (2000 iterations). Fifth row: reconstruction using the proposed model (1000 iterations, $\beta = 30$, $k = .0075$).

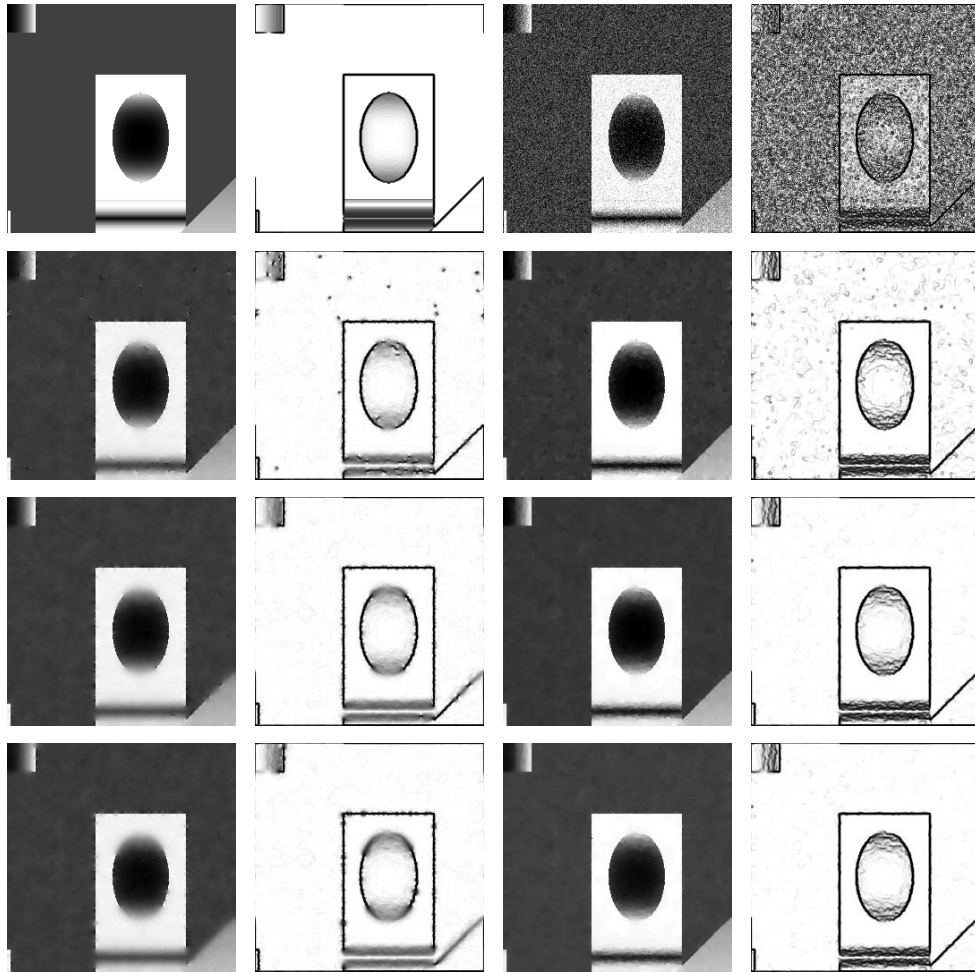


FIG. 5.2. Top row: original piecewise smooth image (256×256) and edge map (5.6), image + noise and edge map (5.6). Bottom three rows: First column from left: reconstructions using (1.2) with thresholds $\beta = 30, 50, 70$, respectively (1000 iterations). Second column: corresponding edge maps (5.6). Third column: reconstruction using TV-based diffusion only (2000 iterations) and the proposed model with thresholds $\beta = 30, 100$, respectively (1000 iterations). Fourth column: corresponding edge maps (5.6) (all images: $k = .0075$, $\lambda = .05$, $\sigma = .5$, time step = .05).

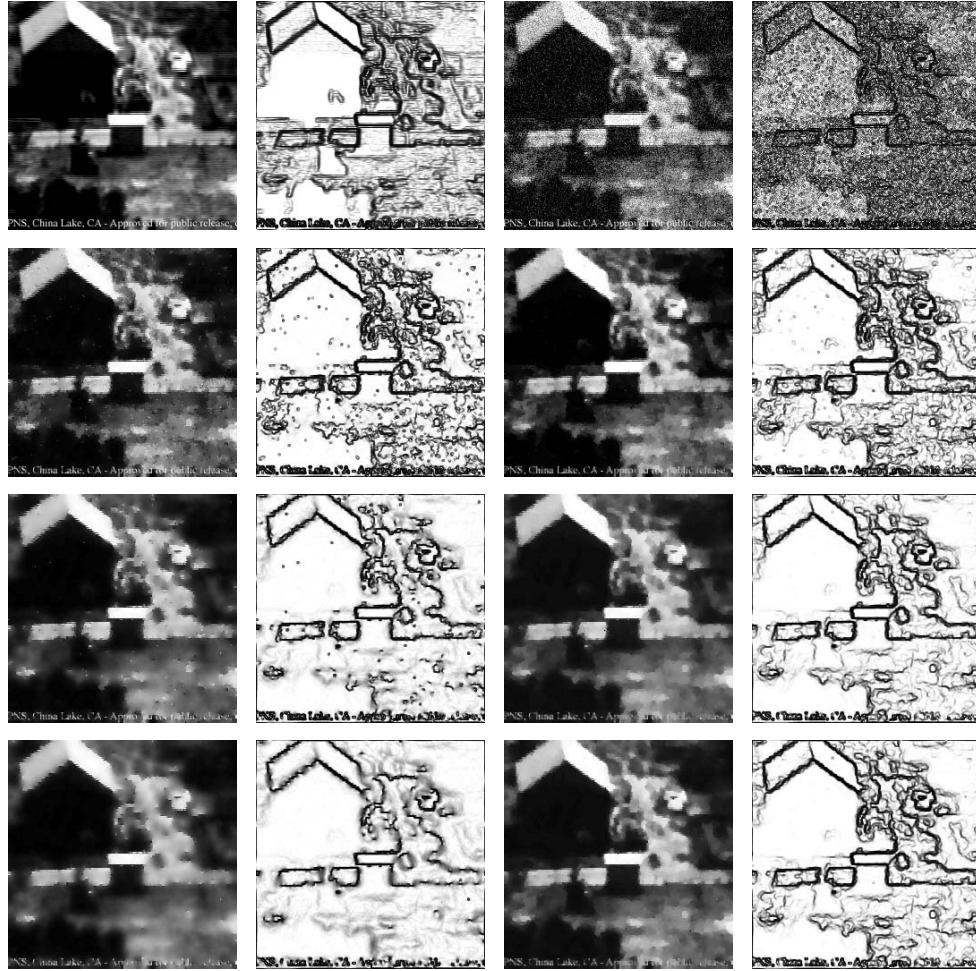


FIG. 5.3. Top row: radar image (256×256) and edge map (5.6); radar image with Gaussian noise and edge map (5.6) with $k = .0075$. Bottom three rows: First column: reconstructions using (1.2) with thresholds $\beta = 10, 20, 30$, respectively (1000 iterations). Second column: corresponding edge maps (5.6). Third column: reconstruction using TV-based diffusion only (4000 iterations) and the proposed model with thresholds $\beta = 30, 100$, respectively (1000 iterations). Fourth column: corresponding edge maps (5.6) (all images: $k = .0075$, $\lambda = .05$, $\sigma = .5$, time step = .05).

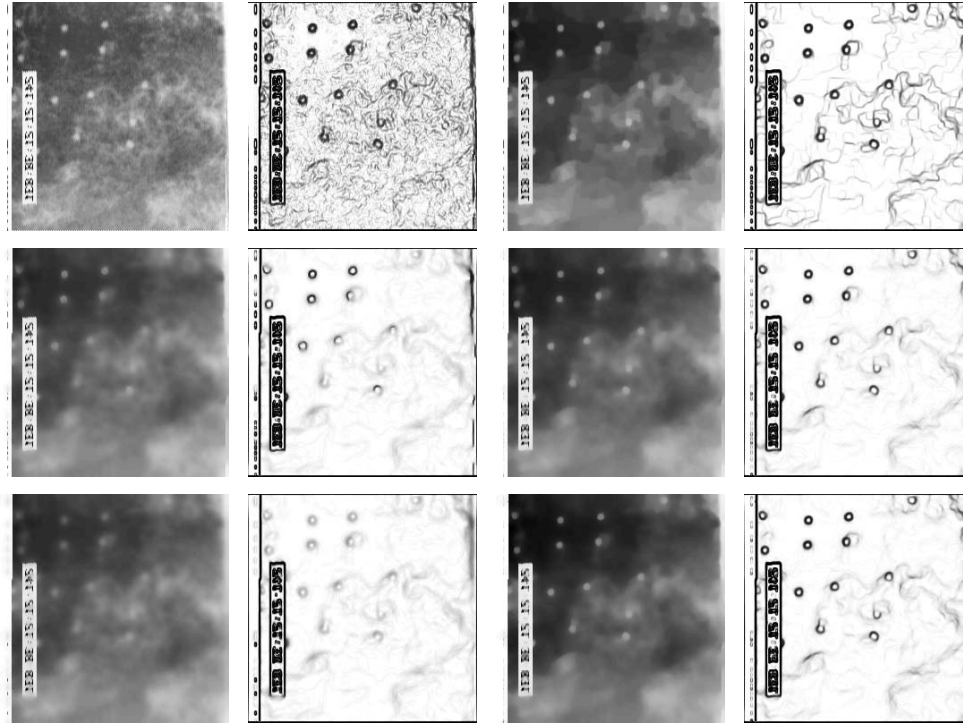


FIG. 5.4. First column from left: radar image of land mines (256×256); reconstructions using (1.2) with thresholds $\beta = 10, 20$, respectively (750 iterations). Second column: corresponding edge maps (5.6). Third column: reconstruction using TV-based diffusion only (1000 iterations); reconstructions using the proposed model with thresholds $\beta = 30, 100$, respectively (750 iterations). Fourth column: corresponding edge maps (5.6) (all images: $k = .0075$, $\lambda = .05$, $\sigma = .5$, time step = .05).

Figure 5.5 provides another successful reconstruction of a piecewise smooth image with additive Gaussian noise. TV-based diffusion alone creates false edges, while the proposed model preserved accurate object boundaries while minimizing the creation of false ones. Tests with $\beta = 30$ and 100 again demonstrate the proposed model's insensitivity to the threshold, β . Figure 5.6 displays a similar experiment with an MRI of a human heart. The original image is successfully denoised using the proposed model (top row). We then added more noise and, as in the previous experiments, found that TV alone created false edges, while the proposed model generated much fewer false artifacts.

Figure 5.7 contains several more examples in which the noise in each of the images was acquired directly through acquisition, storage, or transmission. The first row contains a diffusion tensor image (DTI) of a human brain; the second contains a magnetic resonance image (MRI) of a human chest cavity; the third contains a transmission electron microscope (TEM) image of aluminum. In all of these images, the goal is to detect “true” object boundaries without creating any false edges. The proposed model is successful in all of these cases.



FIG. 5.5. Top row: true image (256×256) and edge map (5.6); true image + noise and edge map (5.6). Second row: reconstructions using TV-based diffusion only (2000 iterations) and the proposed model with thresholds $\beta = 30, 100$ (1000 iterations, $k = .0075$). Third row: corresponding edge maps (5.6) (all images: $k = .0075$, $\lambda = .05$, $\sigma = .5$, time step = .05).

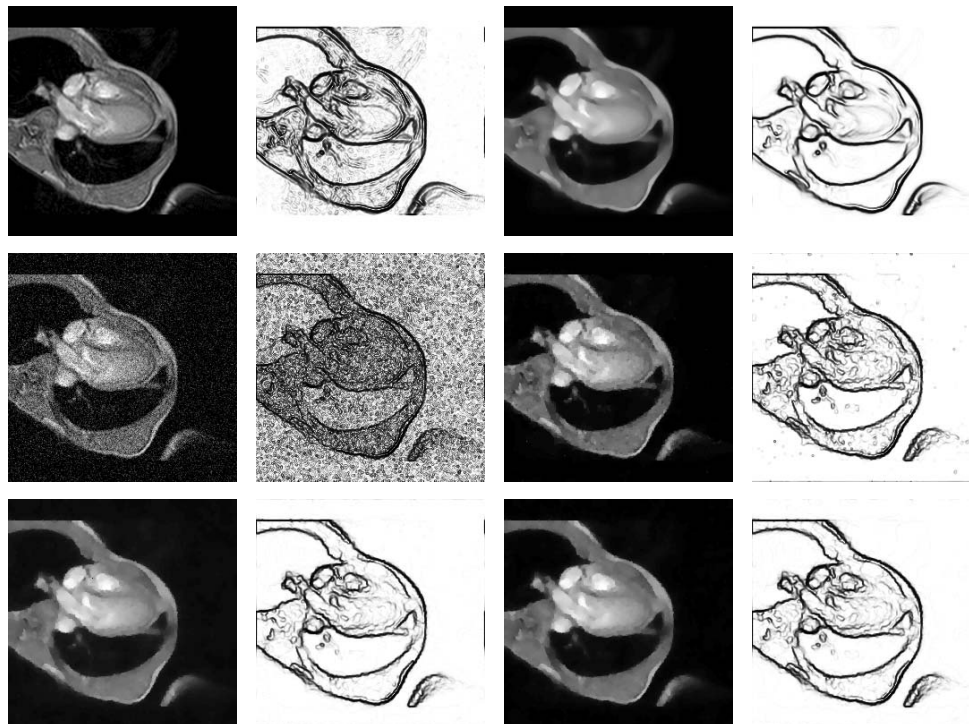


FIG. 5.6. Top row: true image: human heart MRI (256×256), corresponding edge map (5.6), reconstruction using the proposed model (threshold $\beta = 30$), edge map (5.6). Second row: human heart MRI + noise, edge map (5.6), reconstruction using TV-based diffusion only, edge map (5.6). Third row: reconstruction using the proposed model (threshold $\beta = 30$), edge map (5.6), reconstruction using the proposed model (threshold $\beta = 100$), edge map (5.6) (all images: $k = .0075$, $\lambda = .05$, $\sigma = .5$, time step = .05).

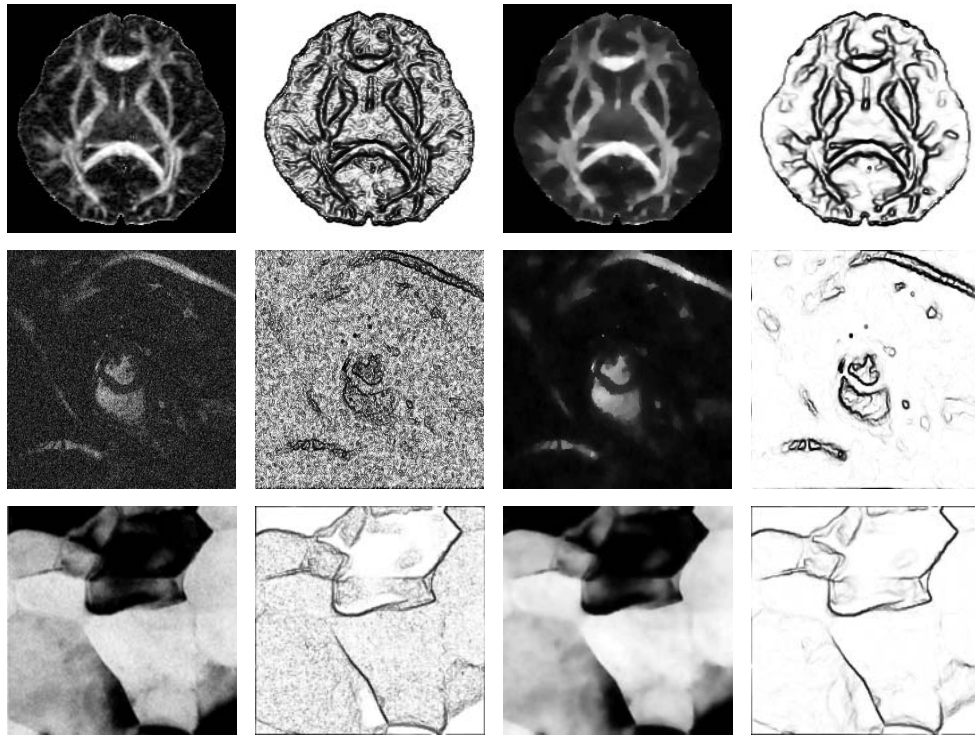


FIG. 5.7. First column from left: true images: human brain DTI (201×171), human chest cavity MRI (209×256), TEM image of aluminum (512×512). Second column: corresponding edge maps (5.6). Third column: reconstructions using the proposed model (420, 1000, 500 iterations, respectively). Fourth column: corresponding edge maps (5.6) with $k = .0075$ (all images: threshold = 30, $k = .0075$, $\lambda = .05$, $\sigma = .5$, time step = .05).

Acknowledgments. The authors would like to thank Bernard Mair for the radar images in Figures 5.3 and 5.4; Sébastien Barre for the MRI in Figure 5.6; and Yijun Liu for the DTI, Mark Griswold for the MRI, and Katayun Barmak for the TEM image in Figure 5.7. We would also like to thank the reviewers for their helpful comments.

REFERENCES

- [1] R. ACAR AND C. R. VOGEL, *Analysis of bounded variation penalty methods for ill-posed problems*, Inverse Problems, 10 (1994), pp. 1217–1229.
- [2] F. ANDREU, C. BALLESTER, V. CASELLES, AND J. M. MAZÓN, *Minimizing total variation flow*, C. R. Acad. Sci. Paris Sér. I Math., 331 (2000), pp. 867–872.
- [3] F. ANDREU, C. BALLESTER, V. CASELLES, AND J. M. MAZÓN, *The Dirichlet problem for the total variation flow*, J. Funct. Anal., 180 (2001), pp. 347–403.
- [4] F. ANDREU, J. M. MAZÓN, J. S. MOLL, AND V. CASELLES, *The minimizing total variation flow with measure initial conditions*, Commun. Contemp. Math., 6 (2004), pp. 431–494.
- [5] F. ANDREU-VAILLO, V. CASELLES, AND J. M. MAZÓN, *Parabolic Quasilinear Equations Minimizing Linear Growth Functionals*, Progr. Math. 223, Birkhäuser Verlag, Basel, 2004.
- [6] G. AUBERT AND L. VESSE, *A variational method in image recovery*, SIAM J. Numer. Anal., 34 (1997), pp. 1948–1979.
- [7] G. BELLETTINI, V. CASELLES, AND M. NOVAGA, *The total variation flow in \mathbb{R}^N* , J. Differential Equations, 184 (2002), pp. 475–525.
- [8] M. BERTALMÍO, G. SAPIRO, V. CASELLES, AND C. BALLESTER, *Image inpainting*, in Proceedings of the 27th Annual Conference on Computer Graphics and Interactive Techniques (SIGGRAPH), ACM Press/Addison Wesley, New York, 2000, pp. 417–424.

- [9] P. BLOMGREN, T. F. CHAN, P. MULET, AND C. WONG, *Total variation image restoration: Numerical methods and extensions*, in Proceedings of the IEEE International Conference on Image Processing, Vol. III, IEEE, Los Alamitos, CA, 1997, pp. 384–387.
- [10] G. BOUCHITTÉ AND G. DAL MASO, *Integral representation and relaxation of convex local functionals on $BV(\Omega)$* , Ann. Scuola Norm. Sup. Pisa Cl. Sci. (4), 20 (1993), pp. 483–533.
- [11] G. BOUCHITTÉ AND M. VALADIER, *Integral representation of convex functionals on a space of measures*, J. Funct. Anal., 80 (1988), pp. 398–420.
- [12] H. BRÉZIS, *Opérateurs maximaux monotones et semi-groupes de contractions dans les espaces de Hilbert*, North-Holland Mathematics Studies 5, Notas de Matemática (50), North-Holland, Amsterdam, 1973.
- [13] V. CASELLES, J.-M. MOREL, AND C. SBERT, *An axiomatic approach to image interpolation*, IEEE Trans. Image Process., 7 (1998), pp. 376–386.
- [14] V. CASELLES, AND L. RUDIN, *Multiscale total variation*, in Proceedings of the Second European Conference on Image Processing (Palma, Spain, September, 1995), pp. 376–386.
- [15] A. CHAMBOLLE AND P.-L. LIONS, *Image recovery via total variation minimization and related problems*, Numer. Math., 76 (1997), pp. 167–188.
- [16] T. CHAN, A. MARQUINA, AND P. MULET, *High-order total variation-based image restoration*, SIAM J. Sci. Comput., 22 (2000), pp. 503–516.
- [17] T. F. CHAN, S. H. KANG, AND J. SHEN, *Euler's elastica and curvature-based inpainting*, SIAM J. Appl. Math., 63 (2002), pp. 564–592.
- [18] T. F. CHAN AND J. SHEN, *Mathematical models for local nontexture inpaintings*, SIAM J. Appl. Math., 62 (2002), pp. 1019–1043.
- [19] Y. CHEN AND M. RAO, *Minimization problems and associated flows related to weighted p energy and total variation*, SIAM J. Math. Anal., 34 (2003), pp. 1084–1104.
- [20] D. C. DOBSON AND F. SANTOSA, *Recovery of blocky images from noisy and blurred data*, SIAM J. Appl. Math., 56 (1996), pp. 1181–1198.
- [21] L. C. EVANS AND R. F. GARIEPY, *Measure Theory and Fine Properties of Functions*, Stud. Adv. Math., CRC Press, Boca Raton, FL, 1992.
- [22] E. GIUSTI, *Minimal Surfaces and Functions of Bounded Variation*, Monogr. Math. 80, Birkhäuser Verlag, Basel, 1984.
- [23] R. HARDT AND X. ZHOU, *An evolution problem for linear growth functionals*, Comm. Partial Differential Equations, 19 (1994), pp. 1879–1907.
- [24] O. A. LADYŽENSKAJA, V. A. SOLONNIKOV, AND N. N. URALCEVA, *Linear and Quasilinear Equations of Parabolic Type*, Transl. Math. Monogr. 23, AMS, Providence, RI, 1967.
- [25] A. LICHNEWSKY AND R. TEMAM, *Pseudosolutions of the time-dependent minimal surface problem*, J. Differential Equations, 30 (1978), pp. 340–364.
- [26] M. LYSAKER, A. LUNDERVOLD, AND X.-C. TAI, *Noise removal using fourth-order partial differential equation with applications to medical magnetic resonance images in space and time*, IEEE Trans. Image Process., 12 (2003), pp. 1579–1590.
- [27] S. MASNOU AND J. M. MOREL, *Level lines based disocclusion*, in Proceedings of the IEEE International Conference on Image Processing (Chicago, IL, October 4–7, 1998), Vol. III, IEEE, Los Alamitos, CA, pp. 259–263.
- [28] M. NIKOLOVA, *Weakly constrained minimization: Application to the estimation of images and signals involving constant regions*, J. Math. Imaging Vision, 21 (2004), pp. 155–175.
- [29] S. OSHER AND J. A. SETHIAN, *Propagating with curvature-dependent speed: Algorithms based on Hamilton–Jacobi formulations*, J. Comput. Phys., 79 (1988), pp. 12–49.
- [30] W. RING, *Structural properties of solutions to total variation regularization problems*, M2AN Math. Model. Numer. Anal., 34 (2000), pp. 799–810.
- [31] L. RUDIN, S. OSHER, AND E. FATEMI, *Nonlinear total variation based noise removal algorithms*, Phys. D, 60 (1992), pp. 259–268.
- [32] D. M. STRONG AND T. F. CHAN, *Spatially and Scale Adaptive Total Variation Based Regularization and Anisotropic Diffusion in Image Processing*, Technical Report CAM96-46, University of California, Los Angeles, CA, 1996. Available online at <http://www.math.ucla.edu/applied/cam/index.html>.
- [33] L. VESE, *A study in the BV space of a denoising-deblurring variational problem*, Appl. Math. Optim., 44 (2001), pp. 131–161.
- [34] R. T. WHITAKER AND S. M. PIZER, *A mult-scale approach to nonuniform diffusion*, Comput. Vision Graph. Image Process. Image Understand., 57 (1993), pp. 99–110.
- [35] Y.-L. YOU AND M. KAVEH, *Fourth-order partial differential equations for noise removal*, IEEE Trans. Image Process., 9 (2000), pp. 1723–1730.
- [36] Y.-L. YOU, W. XU, A. TANNENBAUM, AND M. KAVEH, *Behavioral analysis of anisotropic diffusion in image processing*, IEEE Trans. Image Process., 5 (1996), pp. 1539–1553.
- [37] X. ZHOU, *An evolution problem for plastic antiplanar shear*, Appl. Math. Optim., 25 (1992), pp. 263–285.